Materials Sciences and Applications, 2012, 3, 543-551
http://dx.doi.org/10.4236/msa.2012.38077 Published Online August 2012 (http://www.SciRP.org/journal/msa)

Co-Precipitation Synthesis and Characterization of Nanocrystalline Zinc Oxide Particles Doped with Cu^{2+} Ions

Mergoramadhayenty Mukhtar, Lusitra Munisa, Rosari Saleh*

Departemen Fisika, FMIPA-Universitas Indonesia, Depok, Indonesia.
Email: *rosari.saleh@ui.ac.id

Received May 8th, 2012; revised June 10th, 2012; accepted July 9th, 2012

ABSTRACT

Nanocrystalline Cu-doped ZnO particles were synthesized by the co-precipitation method. The composition, structural, optical and magnetic characterizations were performed by energy dispersive X-Ray spectroscopy, X-Ray diffraction, UV-Visible spectrometer, and vibrating sample magnetometer. The results confirmed that nanocrystalline Cu-doped ZnO particles have a hexagonal wurtzite structure with a high degree of crystallization and a crystallite size of 10 - 16 nm. For Cu above 11 at%, the X-Ray diffraction pattern possessed CuO secondary phase which shows the solubility limit of Cu in the ZnO lattice. Up to 11% at Cu, the presence of Cu in the ZnO lattice as Zn substitution indicated by an in- crease in lattice parameter values. Nanoparticles showed weak ferromagnetic characteristics at room temperature. The absence of secondary phase related to magnetic precipitate shown intrinsic ferromagnetic behaviour.

Keywords: Cu-Doped ZnO; Structural Properties; Room Temperature Ferromagnetism

1. Introduction

Wide band-gap oxide semiconductors, when doped with transition metal ions (Mn, Fe, Co and Ni) have attracted much attention for their promising versatile applications.

ZnO based ferromagnetic semiconductor are paid much attention since the theoretical prediction of room temperature ferromagnetism by Dietl *et al.* in 2000 [1]. They used mean field theory to estimate Currie temperature (T_C) of ferromagnetic semiconductor and they predicted that room temperature ferromagnetism can be created by substituting Mn ion in wide band gap semiconductor such as ZnO or GaN. Due to its wide band gap and exciton binding energy of 60 meV, transition metal doped ZnO is attractive for many UV photonic and transparent electronic applications [2]. Numerous experimental studies have proved the existence of room temperature ferromagnetism in Mn-, Fe-, Co- and Ni-doped ZnO [3-6]. Room temperature ferromagnetism has indeed been reported in many of transition metal-doped ZnO. However, the origin of ferromagnetism in transition metal-doped oxide semiconductors remain controversial, some report claims that the room temperature ferromagnetism in TM-doped oxides might come from precipitation of magnetic cluster or secondary magnetic phases [7,8], while others claims that ferromagnetic ordering is intrinsic [9]. Motivated by these contradictory results, experimental studies have addressed the magnetic properties of Cu-doped, since it is known that the metallic Cu as well as all possible Cu-based oxide such as Cu_2O or CuO is nonmagnetic [10]. Therefore, several scientists suggested that if any ferromagnetism is observed in Cu-based system, then it will undoubtedly be the intrinsic property of the material [11]. However, the experimental results still remain controversial; Buchholz *et al.* [12] nonferromagnetism in *n*-type Cu-doped ZnO sample. On the contrary, other report claimed that, *n*-type Cu-doped ZnO has ferromagnetic behavior [13]. The same results were also found in theoretical studies. Early theoretical investigation showed that ferromagnetic ordering cannot develop in ZnO doped with 25 at% [14]. Later subsequent studies suggested that ZnO doped with low level of Cu concentration should be more succesful in producing ferromagnetism [15-17]. Furthermore, it is shown that the magnetism is very sensitive to the preparation methods and hence preparation conditions, even magnetic properties of Cu-doped ZnO prepared by the same method for the same doping concentration show the lack of reproducibility.

In this paper, we present our investigation to understand the structural and magnetic properties of Cu doped

*Corresponding author.

nanocrystalline ZnO particles prepared through a coprecipitation method. The structural and magnetic properties were correlated to understand the origin of room temperature ferromagnetism in our samples.

2. Experimental

Nanocrystalline Cu-doped ZnO particles in this work were synthesized by co-precipitation process. This method provides advantages, such as low synthesis temperature, small particle and simplicity of processing. The starting materials used in this experiment were copper sulfate monohydrate ($CuSO_4 \cdot 5H_2O$), Zinc sulfate hepta hydrate ($ZnSO_4 \cdot 7H_2O$), 25% aqueous Sodium hydroxide (NaOH) which are all procured from Aldrich and Merck. All of the chemicals used are GR grade without further purification. To synthesize nanocrystalline Cu-doped ZnO particles, two solutions, one containing the requisite amounts of $ZnSO_4 \cdot 7H_2O$ and $CuSO_4 \cdot 5H_2O$ in distilled water, and the other containing 44 mmol NaOH was prepared in 440 ml of de-ionized water. The solution containing $ZnSO_4 \cdot 7H_2O$ and $CuSO_4 \cdot 5H_2O$ was then put into an ordinary ultrasonic cleaner using a 57 kHz operating frequency for 2 h at 50˚C. Then, this solution was subsequently stirred with a magnetic stirrer at 80˚C. The NaOH solution was added until the final pH of the mixed solution reached to 12. The mixed solution was further stirred for 0.5 h with constant stirring. So obtained solution was aged at room temperature for 18 h. This solution was centrifuged and the precipitate that formed was seperated from the solution, and washed several times with ethanol and distilled water in order to remove residual and unwanted impurities. The obtained product was dried in a vacuum oven at 200˚C for 1 h yielding brown Cu-doped ZnO powder.

The composition of the samples was determined by energy dispersive X-Ray spectroscopy (EDX) using scanning microscope. The crystal structure and phase impurity were analysed using X-Ray diffraction (XRD) measurements at room temperature with a standard X-Ray diffractometer Philips PW 1710 and monochromatic Cu-Kα (λ = 1.54060 Å) radiation operated at 40 kV and 20 mA in the range from 10˚ to 80˚. The calibration of the diffractometer was done using Si powder. Structural properties were further studied using Fourier transform infra red (FTIR) measurements. FTIR spectra of the powder samples were recorded using Shimadzu Fourier transform spectrometer. All spectra recorded on pressed pellet of the prepared samples in potassium bromide (KBr) in the range of 400 - 4000 cm^{-1} with resolution of 4 cm^{-1}.

In order to study the electronic interaction near the optical band gap due to addition of dopant atoms UV-Vis diffuse reflectance measurements were deployed. In the present work, measurements have been performed using a Shimadzu UV-Vis spectrophotometer with an integrating sphere attachment and spectralon reflectance standard in the wavelength range of 250 - 800 nm. The diffuse reflectance, R, of the sample is related to the Kubelka-Munk function $F(R)$ by the relation:

$$F(R) = (1 - R)^2/2R$$

The band gap energy of the samples were calculated from the diffuse reflectance spectra by plotting the $F(R)^2$ vs. energy and extrapolated it to $F(R)^2 = 0$.

Magnetic properties were experimentally studied by measuring magnetization as a function of external magnetic field at room temperature using Oxford Type 1.2 T vibrating sample magnetometer (VSM). These measurements were taken from 0 to ±1 Tesla field.

3. Results and Discussion

Figure 1 shows a typical energy dispersive X-Ray (EDX) spectrum of Cu-doped ZnO nanoparticles. In addition to an oxygen peak at 0.53 keV and a Zn signal at 1.01, 8.69 and 9.53 keV, a Cu peak at 8.69 keV was observed. Quantitative results of the Cu/Zn ratio are calculated from the area of the corresponding spectra K lines. The amount of Cu in the nanoparticles has been found to vary between 6 and 23 at%. The inset of **Figure 1** illustrates the Cu incorporation in nanoparticles as a function of the initial cations ratio in the starting solution.

Figure 2 shows the results of XRD patterns of nanocrystalline Cu-doped ZnO, undoped ZnO and CuO particle samples.

The diffraction peak for sample doped with 6 and 11 at% of Cu can be indexed to the hexagonal wurtzite

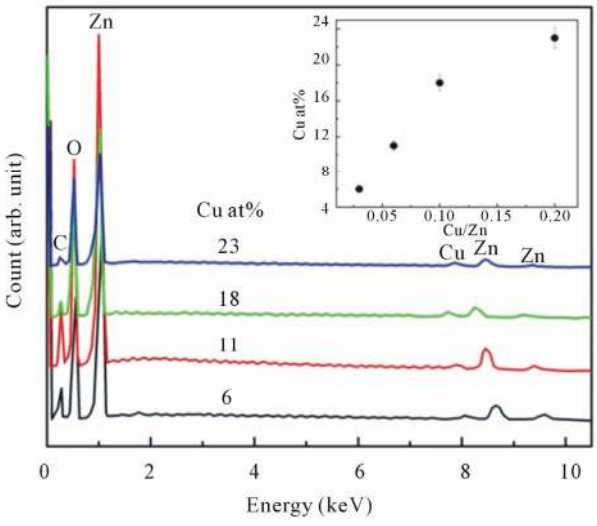

Figure 1. EDX spectra of Cu-doped nanocrystalline ZnO particles for various doping concentrations. For clarity, the spectra are shifted vertically. The inset shows the Cu incorporation in the nanoparticles as a function of the initial cation ratio in the starting solution.

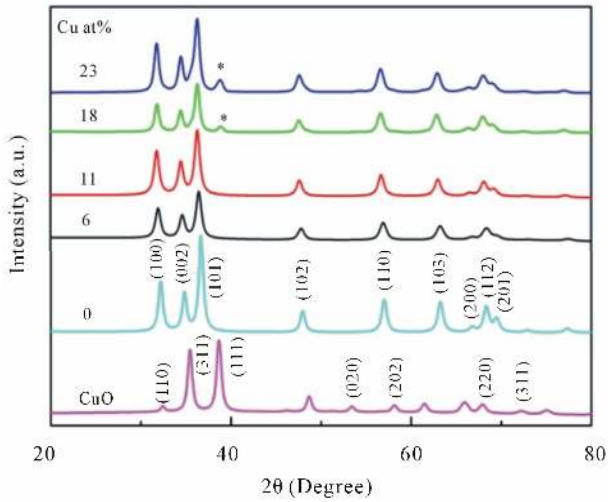

Figure 2. XRD patterns of undoped, CuO and Cu-doped nanocrystalline ZnO particles synthesized with different concentrations of Cu.

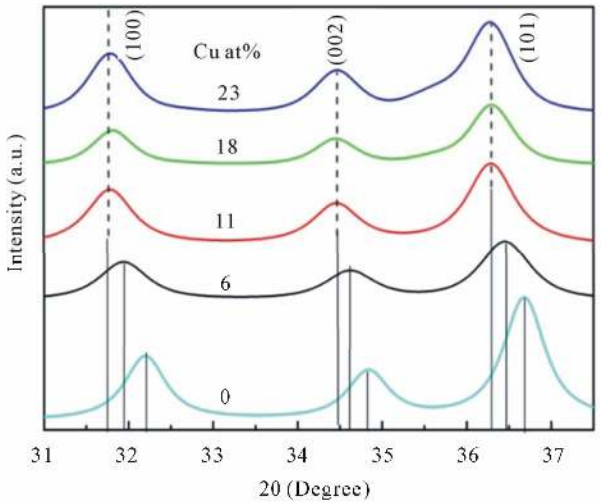

Figure 3. Doping-induced peak shift. This is attributed to Cu^{2+} is replaced in the Zn^{2+} atomic site.

structure of ZnO with nine prominent peaks, clearly suggested that the samples are in single phase within detection limit. No detectable diffraction peak for any secondary or impurity phase such as CuO was found in both samples. Moreover, we can see the Bragg peaks of our Cu-doped ZnO slightly move to lower angle side compared to that of the undoped ZnO sample as shown in **Figure 3**, indicated an important evidence of replacement of Zn^{2+} with Cu^{2+} ions [18].

However, for samples doped with Cu concentration of 18 and 23 at%, reflection (111) of CuO crystalline structure marked by (*) in its corresponding XRD pattern arises. This means a small part of CuO may have been incorporated into the ZnO wurtzite lattice or decompose. This result indicated that the doping limit for our Cu-doped ZnO sample is below 18 at% of Cu. However, there is no noticeable shift in the XRD peak positions towards lower angles for samples doped with 18 and 23 at% compared to samples doped with lower doping concentrations. We have analyzed the effect of doping on the structural changes, such as the lattice parameter, the unit cell volume and average crystallite size. The lattice parameters are estimated from the XRD peaks positions and refined using Rietveld analysis technique. The lattice parameters of undoped ZnO particles were a = 0.3218 nm and c = 0.5155 nm, which is similar with a standard values [19]. For Cu-doped ZnO samples, the lattice parameters are slightly higher than undoped ZnO.

Lattice parameters (a and c), unit cell volume (V), and average crystallite size (<D>) calculated for different doping concentrations are plotted in **Figure 4**. The lattice parameters a, c and V increased with increasing doping concentrations. The unit cell volume continuously increases, which can be explained by looking at the ionic

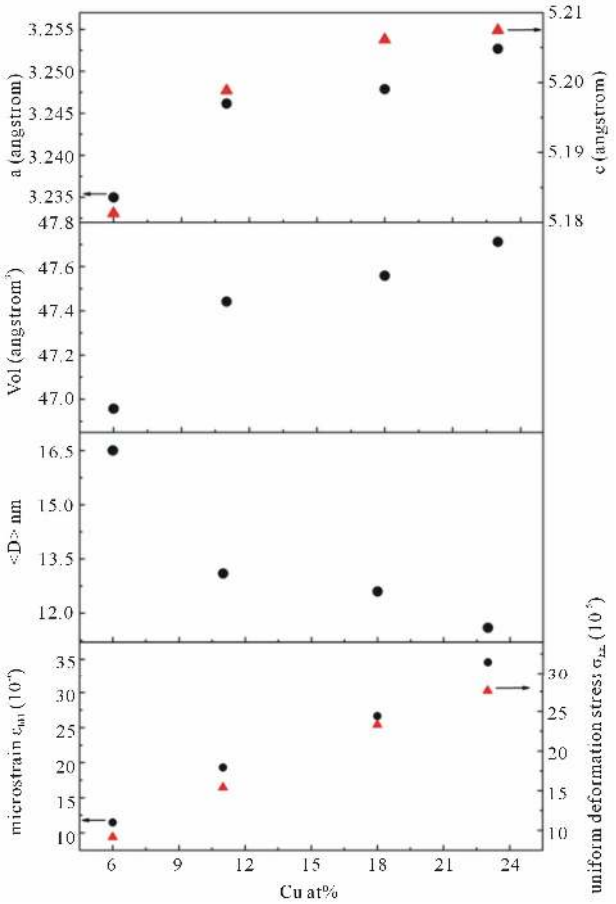

Figure 4. The lattice parameters *a*, *c*, cell volume *V*, average crystallite size and micro strain of Cu-doped nanocrystalline ZnO particles as a function of doping concentration.

radii.

The substitution of the smaller Zn^{2+} ion by the Cu^{2+} ion is expected to result in an expansion of the unit cell

volume. In addition, XRD pattern can be utilized to evaluate lattice strain and stress due to defect or vacancies using Williamson-Hall relation [20]:

$$\Delta_{hkl}\cos\Theta = \kappa\lambda/\langle D\rangle + 4\varepsilon\sin\Theta \quad (1)$$

where k is shape factor (0.89), λ is X-Ray wavelength, Δ_{hkl} is line broadening at half-height, Θ is Bragg angle of the particles and ε is the microstrain.

According to Hooke's law, the stress is proportional to the strain with the constant of proportionality being the modulus of elasticity or Young modulus denoted by Δ_{hkl}. Therefore, as a result, the Equation (1) may be modified as:

$$\Delta_{hkl}\cos\Theta = \kappa\lambda/\langle D\rangle + 4\sin\Theta\sigma/E_{hkl} \quad (2)$$

where σ is the uniform stress. The Equation (2) represents a straight line between $4\sin\Theta\sigma/E_{hkl}$ as an x-axis and $\Delta_{hkl}\cos\Theta$ as an y-axis. The slope of the line gives the uniform stress σ and intercept of this line gives crystallite size <D>. It is observed that the strain in Cu-doped samples varies with doping concentrations. The strain is higher as the dopant is increased. It is seen that more Cu content is introduced into the sample, the stronger tensile is, or more created compression stress is. It is known that the more oxygen vacancies are introduced in the ZnO matrix, the stronger the resulting stress [21]. Accordingly, we believed that our Cu-doped ZnO samples contain oxygen vacancies.

The crystallite size <D> calculated from Williamson and Hall plot was found to decrease with increasing Cu dopant. The average crystallite size was found to be 18 nm for undoped ZnO and 13.45 for the Cu-doped samples, which indicates that the samples are nanocrystalline.

Optical characterization was carried out by measuring the diffuse reflectance at room temperature. All spectra were taken in the range of 200 - 800 nm. The optical gap was estimated from diffuse reflectance spectra by plotting the square of the Kubelka-Munk function $F(R)^2$ given by the relation $F(R) = (1 - R)^2/2R$, where R is the magnitude of reflectance as a function of energy. **Figure 5** shows the $F(R)^2$ as a function of energy for all Cu-doped ZnO samples and to obtained the optical gap the linear part of $F(R)^2$ curve was extrapolated until it intersects the energy axis at $F(R)^2 = 0$. The optical band gap of the various compositions in Cu-doped ZnO samples is shown in **Table 1**. For undoped ZnO the band gap comes out to be 3.4 eV and is in accordance with the

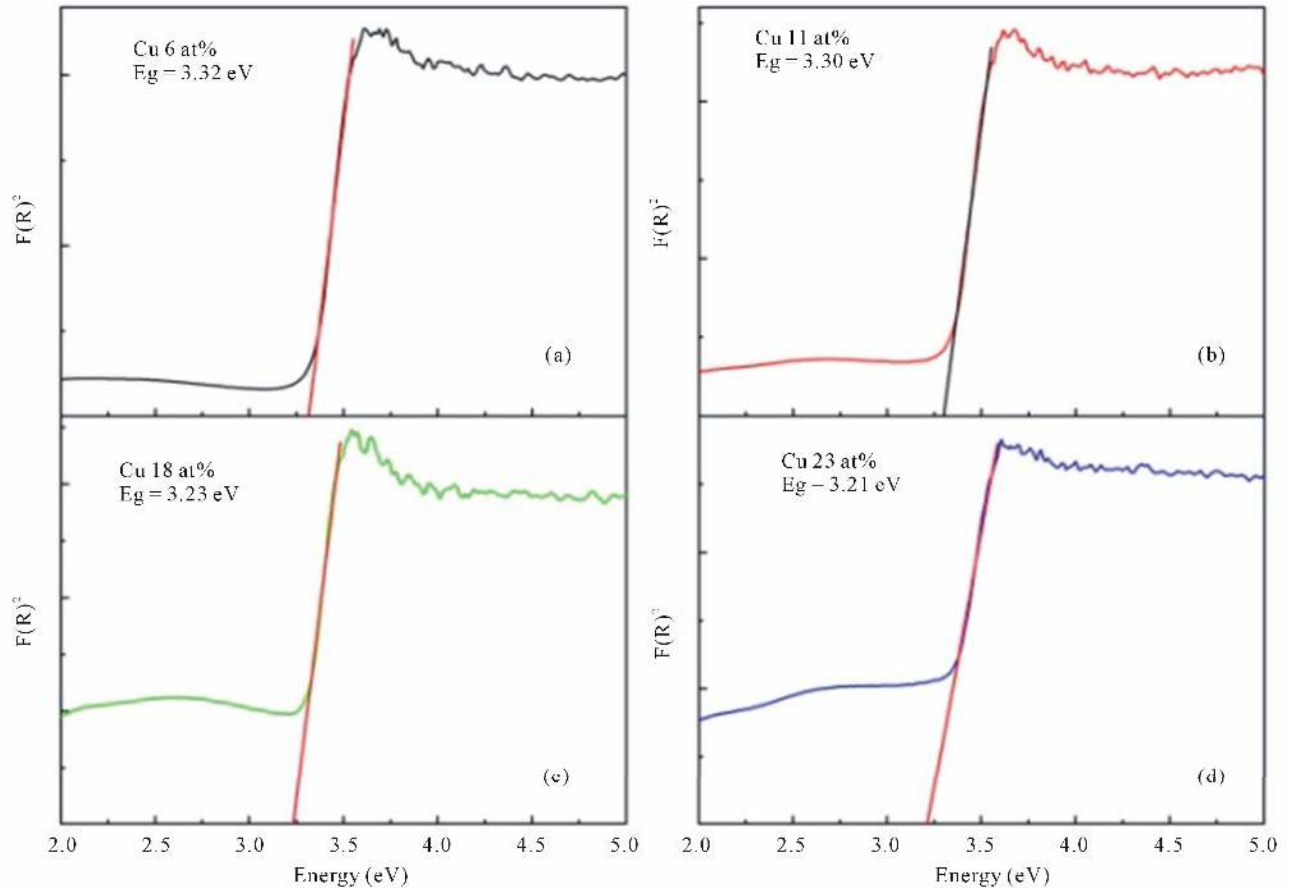

Figure 5. The $F(R)^2$ as a function of energy for all Cu-doped nanocrystalline ZnO particles synthesized with various doping concentrations.

Table 1. Rietveld refined XRD data and optical gap of Cu-doped nanocrystalline ZnO particles.

Sample	at%	a (Å)	c (Å)	V (Å^3)	<D> nm	ε (10^{-4})	Eg (eV)
Cu doped ZnO	0	3.2180	5.1550	47.7017	18.0	10.7	3.46
	6	3.2350	5.1810	46.9570	16.5	11.5	3.32
	11	3.2460	5.1990	47.4420	13.1	19.3	3.30
	18	3.2480	5.2060	47.5590	12.6	26.6	3.23
	23	3.2530	5.2070	47.7120	11.6	34.6	3.21

reported value [22-24]. For Cu-doped ZnO the optical gap was obtained as 3.32, 3.30, 3.23 and 3.21 eV, for doping concentration 6, 11, 18 and 23 at%, respectively.

The band gap is found to decrease with increase Cu concentration in ZnO. Similar mitigation of the band gap with increasing Cu concentration has been reported earlier [25,26]. The inherent reason for red shift in band edge in transition metal doped ZnO samples is due to the change of the sp-d exchange interaction between the band electrons and the localized d-electron of the Cu^{2+} ions [27].

Infrared absorbance spectra are employed to study the vibration bands due to Zn-O bond, the changes due to Cu substitution and hydrogen bonding. Typical infrared absorption spectra of samples synthesized at different doping concentrations are displayed in **Figure 6**. For all Cu-doped samples the strong absorption peaks in the range of 400 - 700 cm^{-1} could be attributed to ZnO stretching modes [28,29]. These stretching modes are indicative of successful synthesized of nanocrystalline ZnO particles as already confirmed by XRD and EDX studies. At the same time we can also observed an absorption peak around 1646, 1390 and 1121 cm^{-1} corresponds to OH bending mode, C-OH plane bending and C-OH out-of-plane bending, respectively [30].

A broad band in the region 2900 - 3700 cm^{-1} can be explained as overlaping of physically absorbed water, O-H stretching modes and C-H stretching modes. C-H local vibrational modes between 2800 and 3100 cm^{-1} have been observed in a number of semiconductor such as amorphous silicon carbon (a-SiC:H), GaAs, and GaN [31-33]. In these materials the local vibrational modes are assigned to symmetric and antisymmetric C-H stretching modes. To obtain information more clearly on the local vibrational modes correspond to OH modes we focalized our analysis on the infrared absorption range of interest, namely in a wave number range of 2900 - 3700 cm^{-1}.

All spectra can be deconvoluted into two peaks around 2990 cm^{-1} attributed to CH stretching mode and 3400 cm^{-1} associated with physically absorbed water and O-H stretching modes (dashed line in **Figure 7**). The integrated absorption is evaluated using the sum of the absorption areas from the fits data. As the dopant concentration is increased, the integrated absorption of the OH and CH stretching modes appears to be independent of

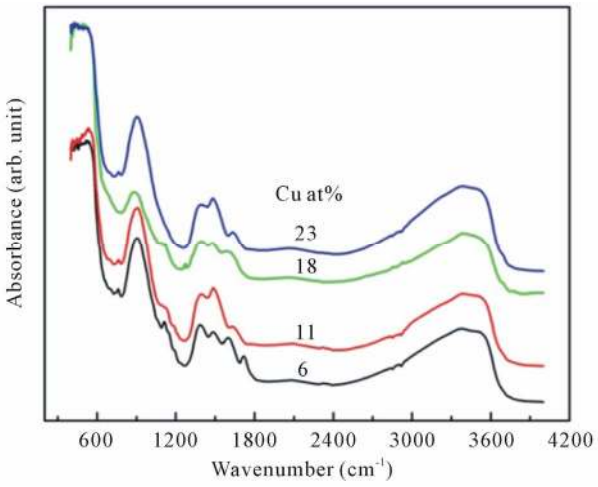

Figure 6. The infrared spectra of Cu-doped nanocrystalline ZnO particles synthesized with various doping concentrations.

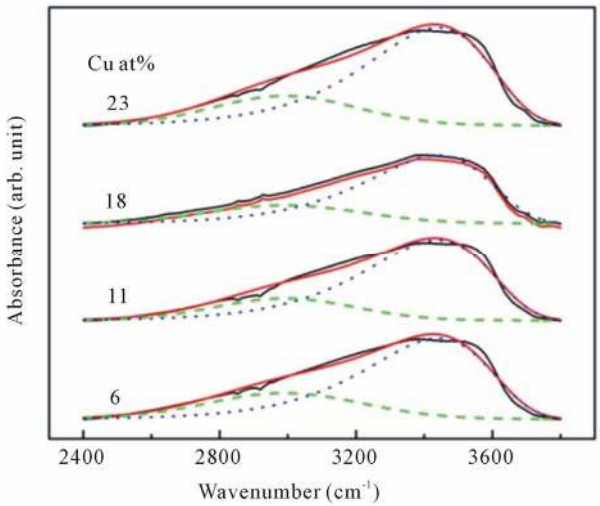

Figure 7. Representative deconvolution of C-H stretching (dash line) and O-H stretching (dotted line) modes of infrared absorption band in the range of 2400 - 3900 cm^{-1} for Cu-doped ZnO nanoparticles.

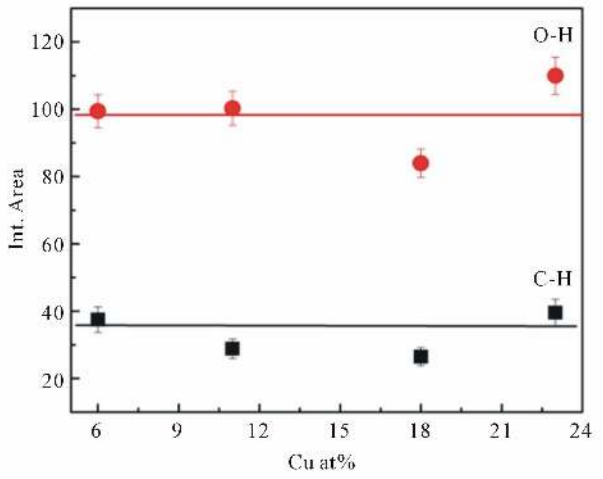

Figure 8. Integrated absorption of C-H stretching mode at 2990 cm^{-1} and O-H stretching mode at 3400 cm^{-1}.

the dopant concentrations in the samples (**Figure 8**).

The magnetization as a function of magnetic field (M-H loop) measured at room temperature for samples doped with 6, 11, 18 and 23 at% of Cu are studied using VSM in the applied magnetic field range of 0 - 1 T. The maximum value of magnetic moment per Cu atom increased with increasing dopant atoms.

The corresponding curves are shown in **Figure 9** reveal the dependence of magnetization on the applied magnetic field for all doped samples. The inset of **Figure 9** clearly displays the magnetization data with an open loop for all Cu-doped samples. The variation in saturation magnetization, remnant magnetization and coercivity for different Cu-doped samples is presented in **Table 2**. However, the magnetization values are much smaller than the 1 μ_B/Cu expected for Cu^{2+} ions homogenously dispersed in the ZnO bulk.

Since Cu and related oxides are nonmagnetic materials at room temperature, the observed ferromagnetism is thought to be intrinsic properties of the Cu-doped ZnO [34]. A similar result was also found by Sharma *et al.* [35]. Sudakar *et al.* [36] reported that Cu-doped ZnO films with concentration lower than 1 at% exhibited ferromagnetic behavior with large saturation magnetization, however, for higher doping concentrations, the saturation magnetization decreased drastically. They proposed that

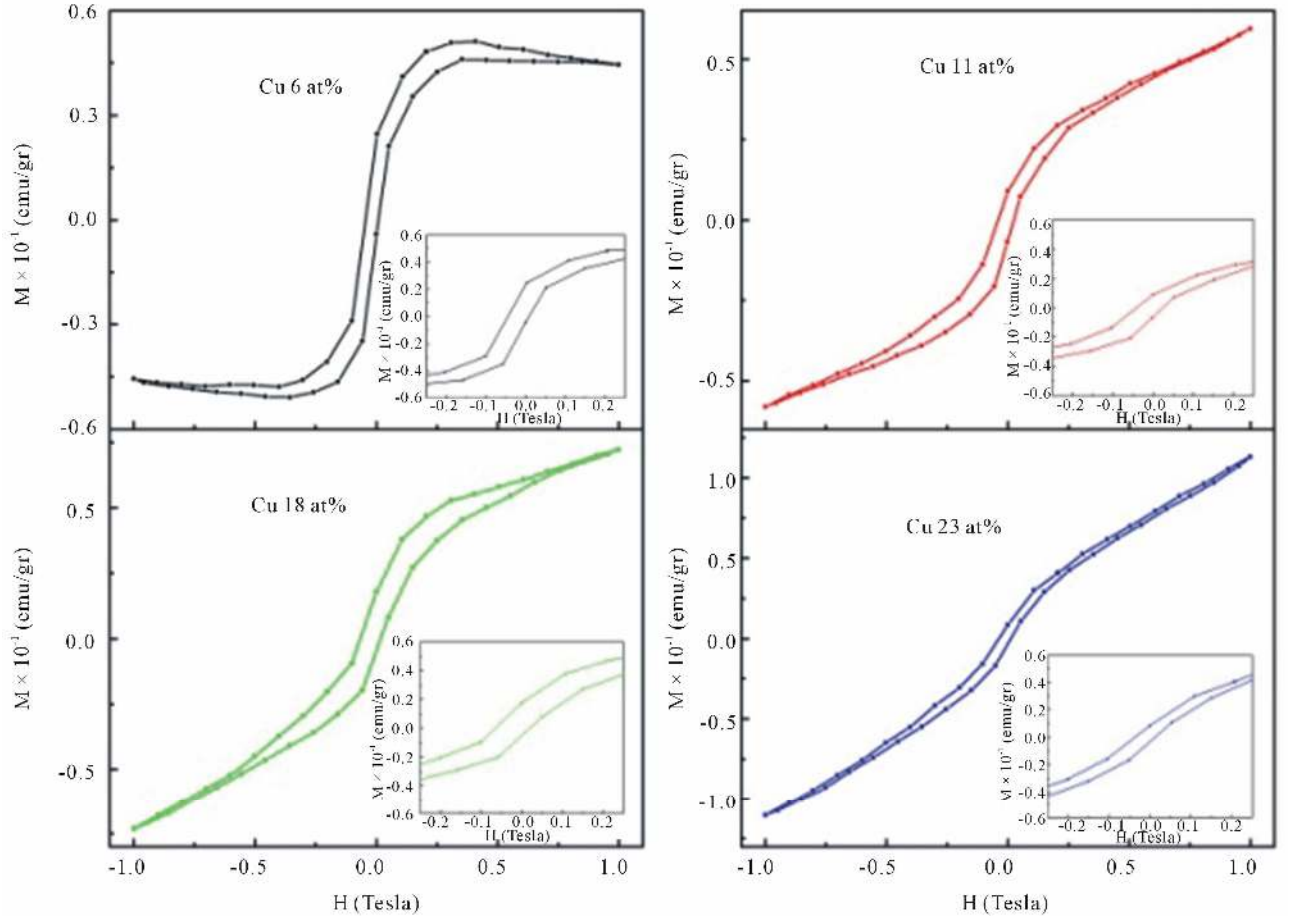

Figure 9. Room temperature M-H curves for Cu-doped nanocrystalline ZnO particles synthesized with various doping concentrations.

Table 2. Magnetization value, remanence magnetization, and coercivity of Cu-doped nanocrystalline ZnO particles.

Sample	at%	μ_B/Cu^{2+}	H_C (oe)	$M_R \times 10^{-2}$ (emu/gr)
Cu doped ZnO	6	0.1008	270	1.39
	11	0.1512	329	0.77
	18	0.1862	415	1.14
	23	0.2318	235	0.57

the origin of ferromagnetism in Cu-doped ZnO was the formation of planar CuO nanophase, while Wei *et al.* [37] reported that there was no sign of ferromagnetism down to 10 K in pure Cu_2O samples. Seehra *et al.* [38], on the other hand suggested that the CuO phase is paramagnet in the $Cu_xZn_{1-x}O$/CuO composite. Tong *et al.* [39], and Wang *et al.* [40] showed, that hydrogen incorporation in the sample can induced ferromagnetism. They believed, that hydrogen as shallow donor might be responsible for the enhancement of RTFM. Hydrogen induces RTFM, however, may not be valid in the present study because the detailed results of FTIR measurements clearly showed that hydrogen incorporation in our doped samples is almost independent with doping concentrations, indicating that hydrogen is not expected to play a crucial role in activating ferromagnetic behavior in our samples.

Chakraborti *et al.* [41] showed in their experiment that the effective moment per Cu atom is found to be very high for the lowest dopant concentrations of Cu and proposed that oxygen vacancies are the origin of ferromagnetism in Cu-doped ZnO films, while theoretical study by Ye *et al.* [42] reported that oxygen vacancies tend to destroy the ferromagnetism in Cu-doped ZnO. However, a similar correlation between oxygen vacancy concentration and ferromagnetic behavior have been observed in several oxide-based dilute magnetic semiconductor materials such as Fe-doped SnO_2 [43], Co doped TiO_2 [44], Co doped CeO_2 [45], Ni- and Mn-doped ZnO [46,47].

A defect mediated mechanism namely a bound magnetic polaron (BMP) [48] has been suggested as being responsible for the ferromagnetism in these systems. According to BMP model, bound electrons in defects like oxygen vacancies, can couple with Cu ions and cause ferromagnetic regions to overlap giving rise to long range ferromagnetic ordering in the samples.

From the energy band point of view, the BMP overlap to produce spin-split impurity band [49], and the electrons are able to transfer from the BMP impurity band to an unoccupied 3 d state of Cu ions at the Fermi level. Therefore, the ferromagnetism of the system will be established.

4. Summary

Cu-doped nanocrystalline ZnO particles have been synthesized using the co-precipitation method and based on the structural, optical and magnetic measurements of our samples the following main point emerge:

1) Structure analysis indicates that Cu ions substitute for Zn ions without changing the wurtzite structure. The determined solubility limit of Cu in nanocrystalline ZnO particles by XRD studies is approximately 11 at%.

2) The optical band gap was found to decrease with increasing doping concentrations, indicating a clear red shift.

3) All samples were found to exhibit ferromagnetic ordering at room temperature. The magnetization results showed that the ferromagnetism behavior is the intrinsic behavior.

4) The infrared absorption measurements showed clear evidence of hydrogen incorporation in our nanocrystalline ZnO particles. It is possible that hydrogen could induce ferromagnetism in our samples. Unfortunately, we do not have experimental evidence of the spin-spin interaction due to the incorporation of hydrogen atoms, and such analysis is beyond the scope of our work.

REFERENCES

[1] T. Dietl, H. Ohno and F. Matsukura, "Hole-Mediated Ferromagnetism in Tetrahedrally Coordinated Semiconductors," *Physical Review B*, Vol. 63, 2001, Article ID: 195205. doi:10.1103/PhysRevB.63.195205

[2] D. Chakraborti, G. R. Trichy, J. T. Prater and J. Narayan, "The Effect of Oxygen Annealing on ZnO:Cu and ZnO:(Cu, Al) Diluted Magnetic Semiconductors," *Journal of Physics D*: *Applied Physics*, Vol. 40, No. 24, 2007, p. 7606. doi:10.1088/0022-3727/40/24/002

[3] S. Venkataraj, N. Ohash1, I. Sakaguchi, Y. Adachi, T. Ohgaki, H. Ryoken and H. Haneda, "Structural and Magnetic Properties of Mn-Ion Implanted ZnO Films," *Journal of Applied Physics*, Vol. 102, No. 1, 2007, Article ID: 014905. doi:10.1063/1.2752123

[4] S.-J. Han, J. W. Song, C.-H. Yang, S. H. Park, J.-H. Park, Y. H. Jeong and K. W. Rhie, "A Key to Room-Temperature Ferromagnetism in Fe-Doped ZnO:Cu," *Applied Physics Letters*, Vol. 81, No. 22, 2002, pp. 4212-4214. doi:10.1063/1.1525885

[5] K. Ueda, H. Tabata and T. Kawai, "Magnetic and Electric Properties of Transition-Metal-Doped ZnO Films," *Applied Physics Letters*, Vol. 79, No. 7, 2001, pp. 988-990.

doi:10.1063/1.1384478

[6] T. Wakano, N. Fujimura, Y. Morinaga, N. Abe, A. Ashida and T. Ito, "Magnetic and Magneto-Transport Properties of ZnO:Ni Films," *Physica E*: *Low-Dimensional Systems and Nanostructures*, Vol. 10, No. 1-3, 2001, pp. 260-264. doi:10.1016/S1386-9477(01)00095-9

[7] S. J. Han, T. H. Jang, Y. B. Kim, B. G. Park, J. H. Park and Y. H. Jeong, "Magnetism in Mn-Doped ZnO Bulk Samples Prepared by Solid State Reaction," *Applied Physics Letters*, Vol. 83, No. 5, 2003, pp. 920-922. doi:10.1063/1.1597414

[8] D. C. Kundaliya, S. B. Ogale, S. E. Lofland, S. Dhar, C. J. Metting, S. R. Shinde, Z. Ma, B. Varughese, K. V. Ramanujachari, L. Salamanca-Riba and T. Venkatesan, "On the Origin of High-Temperature Ferromagnetism in the Low-Temperature-Processed Mn-Zn-O System," *Nature Matter*, Vol. 3, No. 10, 2004, pp. 709-714. doi:10.1038/nmat1221

[9] H. L. Liu, J. H. Yang, Z. Hua, Y. J. Zhang, L. L. Yang, L. Xiao and Z. Xie, "The Structure and Magnetic Properties of Cu-Doped ZnO Prepared by Sol-Gel Method," *Applied Surface Science*, Vol. 256, No. 13, 2010, pp. 4162-4165.

[10] T. S. Herng, S. P. Lau, S. F. Yu, H. Y. Yang, X. H. Ji, J. S. Chen, N. Yasui and H. Inaba, "Origin of Room Temperature Ferromagnetism in ZnO:Cu Films," *Journal of Applied Physics*, Vol. 99, No. 8, 2006, Article ID: 086101. doi:10.1063/1.2190711

[11] A. Tiwari, M. Snure, D. Kumar and J. T. Abiade, "Ferromagnetism in Cu-Doped ZnO Films: Role of Charge Carriers," *Applied Physics Letters*, Vol. 92, No. 6, 2008, Article ID: 062509. doi:10.1063/1.2857481

[12] D. B. Buchholz, R. P. H. Chang, J.-Y. Song and J. B. Ketterson, "Room-Temperature Ferromagnetism in Cu-Doped ZnO Thin Films," *Applied Physics Letters*, Vol. 87, No. 8, 2005, Article ID: 082504. doi:10.1063/1.2032588

[13] L.-H. Ye, A. J. Freeman and B. Delley, "Half-Metallic Ferromagnetism in Cu-Doped ZnO: Density Functional Calculations," *Physical Review B*, Vol. 73, 2006, Article ID: 033203. doi:10.1103/PhysRevB.73.033203

[14] K. Sato and H. Katayama-Yoshida, "Microdischarge Optical Emission Spectroscopy as a Novel Diagnostic Tool for Metalorganic Chemical Vapor Deposition of (Ba, Sr)TiO_3 Films," *JJAP*: *Japanese Journal of Applied Physics*, Vol. 39, 2000, pp. 555-559. doi:10.1143/JJAP.39.555

[15] D. L. Hou, X. J. Ye, H. J. Meng, H. J. Zhou, X. L. Li, C. M. Zhen and G. D. Tang, "Magnetic Properties of *n*-Type Cu-Doped ZnO Thin Films," *Applied Physics Letters*, Vol. 90, No. 14, 2007, Article ID: 142502. doi:10.1063/1.2719034

[16] M. S. Park and B. I. Min, "Ferromagnetism in ZnO Codoped with Transition Metals: $Zn_{1-x}(FeCo)_xO$ and $Zn_{1-x}(FeCu)_xO$," *Physical Review B*, Vol. 68, 2003, Article ID: 224436.

[17] S. W. Jung, S-J. An, G.-C. Yi, C.-U. Jung, S.-I. Lee and S. Cho, "Ferromagnetic Properties of $Zn_{1-x}Mn_xO$ Epitaxial Thin Films," *Applied Physics Letters*, Vol. 80, No. 4, 2002, pp. 4561-4563. doi:10.1063/1.1487927

[18] U. Ilyas, R. S. Rawat, T. L. Tan, P. Lee, R. Chen, H. D. Sun, F. J. Li and S. Zhang, "Enhanced Indirect Ferromagnetic p-d Exchange Coupling of Mn in Oxygen Rich ZnO:Mn Nanoparticles Synthesized by Wet Chemical Method," *Journal of Applied Physics*, Vol. 111, No. 3, 2012, Article ID: 033503. doi:10.1063/1.3679129

[19] S. P. Prakoso and R. Saleh, "Hydrogen Incorporation in Undoped ZnO Nanoparticles," *World Journal of Condensed Matter Physics*, Vol. 1, No. 4, 2011, pp. 130-136. doi:10.4236/wjcmp.2011.14019

[20] G. K. Williamson and W. H. Hall, "X-Ray Line Broadening from Filled Aluminium and Wolfram," *Acta Metallurgica*, Vol. 1, No. 1, 1953, pp. 22-31. doi:10.1016/0001-6160(53)90006-6

[21] A. Janotti and C. G. Van de Walle, "Oxygen Vacancies in ZnO," *Applied Physics Letters*, Vol. 87, No. 12, 2005, Article ID: 122102. doi:10.1063/1.2053360

[22] R. Viswanatha, S. Chakraborty, S. Basu and D. D Sarma, "Blue-Emitting Copper-Doped Zinc Oxide Nanocrystals," *The Journal of Physical Chemistry B*, Vol. 110, No. 45, 2006, pp. 22310-22312.

[23] R. Viswanatha, S. Sapra, B. Satpati, P. V. Satyam, B. N. Dev and D. D. Sarma, "Understanding the Quantum Size Effects in ZnO Nanocrystals," *Journal of Materials Chemistry*, Vol. 14, 2004, pp. 661-668.

[24] P. Sharma, A. Gupta, K. V. Rao, F. J. Owens, R. Sharma, R. Ahuja, J. M. Osorio, B. Johansson and G. A. Gehring, "Ferromagnetism above Room Temperature in Bulk and Transparent Thin Films of Mn-Doped ZnO," *Nature Matter*, Vol. 2, 2003, pp. 673-677. doi:10.1038/nmat984

[25] A. Jagannatha Reddy, M. K. Kokila, H. Nagabhushana, R. P. S. Chakradhar, C. Shivakumara, J. L. Rao and B. M. Nagabhushana, "Structural, Optical and EPR Studies on ZnO:Cu Nanopowders Prepared via Low Temperature Solution Combustion Synthesis," *Journal of Alloys and Compounds*, Vol. 509, No. 17, 2011, pp. 5349-5355. doi:10.1016/j.jallcom.2011.02.043

[26] Y. Chen and X. L. Xu, "Effect of Oxygen Deficiency on Optical Band Gap Shift in Er-Doped ZnO Thin Films," *Physica B*: *Condensed Matter*, Vol. 406, No. 17, 2011, pp. 3121-3124. doi:10.1016/j.physb.2011.03.078

[27] K. G. Kanade, B. B. Kale, J.-O. Baeg, S. M. Lee, C. W. Lee, S.-J. Moon and H. Chang, "Self-Assembled Aligned Cu Doped ZnO Nanoparticles for Photocatalytic Hydrogen Production under Visible Light Irradiation," *Materials Chemistry and Physics*, Vol. 102, No. 1, 2007, pp. 98-104. doi:10.1016/j.matchemphys.2006.11.012

[28] M. Y. Ghotbi, N. Bagheri and S. K. Sadrnezhaad, "Nanocrystalline Copper Doped Zinc Oxide Produced from Copper Doped Zinc Hydroxide Nitrate as a Layered Precursor," *Advanced Powder Technology*, Vol. 23, No. 3, 2012, pp. 279-283.

[29] H. Kleinwechter, C. Janzen, J. Knipping, H. Wiggers and P. Roth, "Formation and Properties of ZnO Nano-Particles from Gas Phase Synthesis Processes," *Journal of Materials Science*, Vol. 37, No. 20, 2002, pp. 4349-4360. doi:10.1023/A:1020656620050

[30] J. Das, I. R. Evans and D. Khushalani, "Zinc Glycolate: A Precursor to ZnO," *Inorganic Chemistry*, Vol. 48, No. 8, 2009, pp. 3508-3510. doi:10.1021/ic900067w

[31] R. Saleh, L. Munisa and W. Beyer, "Infrared Absorption in a-SiC:H Alloy Prepared by d.c Sputtering," *Thin Solid Films*, Vol. 426, No. 1, 2003, pp. 117-123. doi:10.1016/S0040-6090(03)00003-8

[32] D. M. Joseph, R. Balagopal, R. F. Hicks, L. P. Sadwick and K. L. Wang, "Observation of Carbon Incorporation during Gallium Arsenide Growth by Molecular Beam Epitaxy," *Applied Physics Letters*, Vol. 53, No. 22, 1988, pp. 2203-2204. doi:10.1063/1.100281

[33] M. O. Manasreh, J. M. Baranowski, K. Pakula, H. X. Jiang and J. Lin, "Localized Vibrational Modes of Carbon-Hydrogen Complexes in GaN," *Applied Physics Letters*, Vol. 75, No. 5, 1999, pp. 659-661. doi:10.1063/1.124473

[34] P. Thakur, V. Bisogni, J. C. Cezar, N. B. Brookes, G. Ghiringhelli, S. Gautam, K. H. Chae, M. Subramanian, R. Jayavel and K. Asokan, "Electronic Structure of Cu-Doped ZnO Thin Films by X-Ray Absorption, Magnetic Circular Dichroism, and Resonant Inelastic X-Ray Scattering," *Journal of Applied Physics*, Vol. 107, 20110, Article ID: 103915.

[35] P. K. Sharma, R. K. Dutta and A. C. Pandey, "Doping Dependent Room-Temperature Ferromagnetism and Structural Properties of Dilute Magnetic Semiconductor ZnO: Cu^{2+} Nanorods," *Journal of Magnetism and Magnetic Materials*, Vol. 321, No. 24, 2009, pp. 4001-4005. doi:10.1016/j.jmmm.2009.07.066

[36] C. Sudakar, J. S. Thakur, G. Lawes, R. Naik and V. M. Naik, "Ferromagnetism Induced by Planar Nanoscale CuO Inclusions in Cu-Doped ZnO Thin Films," *Physical Review B*, Vol. 75, 2007, Article ID: 054423. doi:10.1103/PhysRevB.75.054423

[37] M. Wei, N. Braddon, D. Zhi, P. A. Midgley, S. K. Chen, M. G. Blamire and J. L. MacManus-Driscoll, "Room Temperature Ferromagnetism in Bulk Mn-Doped Cu_2O," *Applied Physics Letters*, Vol. 86, No. 7, 2005, Article ID: 072514. doi:10.1063/1.1869547

[38] M. S. Seehra, P. Dutta, V. Singh, Y. Zhang and I. Wender, "Evidence for Room Temperature Ferromagnetism in $Cu_xZn_{1-x}O$ from Magnetic Studies in $Cu_xZn_{1-x}O$/CuO Composite," *Journal of Applied Physics*, Vol. 101, No. 9, 2007, Article ID: 09H107.

[39] L. N. Tong, T. Cheng, H. B Han, J. L. Hu, X. M. He, Y. Tong and C. M. Schneider, "Photoluminescence Studies on Structural Defects and Room Temperature Ferromagnetism in Ni and Ni-H Doped ZnO Nanoparticles," *Journal of Applied Physics*, Vol. 108, 2010, Article ID: 023906.

[40] Z. H. Wang, D. Y. Geng, S. Guo, W. J. Hu and Z. D. Zhang, "Ferromagnetism and Superparamagnetism of ZnCoO:H Nanocrystals,"*Applied Physics Letters*, Vol. 92, No. 24, 2008, Article ID: 242505. doi:10.1063/1.2948863

[41] D. Chakraborti, J. Narayan and J. T. Prater, "Room Temperature Ferromagnetism in $Zn_{1-x}Cu_xO$ Thin Films," *Applied Physics Letters*, Vol. 90, No. 8, 2007, Article ID: 062504. doi:10.1063/1.2450652

[42] L.-H. Ye, A. J. Freeman and B. Delley, "Half-Metallic Ferromagnetism in Cu-Doped ZnO: Density Functional Calculations," *Physical Review B*, Vol. 73, 2006, Article ID: 033203. doi:10.1103/PhysRevB.73.033203

[43] J. M. D. Coey, A. P. Douvalis, C. B. Fitzgerald and M. Venkatesan, "Ferromagnetism in Fe-Doped SnO_2 Thin Films," *Applied Physics Letters*, Vol. 84, No. 8, 2004, pp. 1332-1334. doi:10.1063/1.1650041

[44] W. S. Yan, Z. H. Sun, Z. Y. Pan, Q. H. Liu, T. Yao, Z. Y. Wu, C. Song, F. Zeng, Y. Xie, T. D. Hu and S. Q. Wei, "Oxygen Vacancy Effect on Room-Temperature Ferromagnetism of Rutile Co:TiO_2 Thin Films," *Applied Physics Letters*, Vol. 94, No. 4, 2009, Article ID: 042508. doi:10.1063/1.3075844

[45] Y.-Q. Song, H.-W. Zhang, Q.-Y. Wen, L. Peng and J. Q. Xiao, "Direct Evidence of Oxygen Vacancy Mediated Ferromagnetism of Co Doped CeO_2 Thin Films on Al_2O_3 (0001) Substrates," *Journal of Physics*: *Condensed Matter*, Vol. 20, No. 25, 2008, Article ID: 255210. doi:10.1088/0953-8984/20/25/255210

[46] M. El-Hilo, A. A. Dakhel and A. Y. Ali-Mohamed, "Room Temperature Ferromagnetism in Nanocrystalline Ni-Doped ZnO Synthesized by Co-Precipitation," *Journal of Magnetism and Magnetic Materials*, Vol. 321, No. 14, 2009, pp. 2279-2283. doi:10.1016/j.jmmm.2009.01.040

[47] Z. H. Wang, D. Y. Geng and Z. D. Zhang, "Room-Temperature Ferromagnetism and Optical Properties of $Zn_{1-x}Mn_xO$ Nanoparticles," *Solid State Communication* Vol. 149, No. 17-18, 2009, pp. 682-684. doi:10.1016/j.ssc.2009.02.016

[48] D. Chakraborti, G. Trichy, J. Narayan, J. T. Prater and D. Kumar, "Effect of Al Doping on the Magnetic and Electrical Properties of Zn(Cu)O Based Diluted Magnetic Semiconductors," *Journal of Applied Physics*, Vol. 102, No. 11, 2007, Article ID: 113908. doi:10.1063/1.2817824

[49] J. J. Lu, T. C. Lin, S. Y. Tsai, T. S. Mo and K. J. Gan, "Structural, Magnetic and Transport Properties of Ni-Doped ZnO Films," *Journal of Magnetism and Magnetic Materials*, Vol. 323, No. 6, 2011, pp. 829-832. doi:10.1016/j.jmmm.2010.11.025

